Electronic Supplementary Material (ESI) for Chemical Communications.
This journal is © The Royal Society of Chemistry 2017

Supporting information

Control of Bulk Homochirality and Proton Conductivity in Isostructural Chiral Metal-organic Frameworks

Bai-Qiao Song,[ab] Da-Qin Chen,[b] Zhenguo Ji,[b] Junhong Tang,[b] Xin-Long Wang,*[a] Hong-Ying Zang,[a] and Zhong-Min Su*[a]

[a]Institute of Functional Material Chemistry, Local United Engineering Lab for Power Battery, Northeast Normal University, Changchun, 130024 Jilin, People's Republic of China. E-mail: wangxl824@nenu.edu.cn, zmsu@nenu.edu.cn; Fax: + 86 431-85684009; Tel: + 86 431-85099108.
[b]College of Materials & Environmental Engineering, Hangzhou Dianzi University, Hangzhou, 310018 Zhejiang, People's Republic of China.

S1. Materials and Measurements

Chemicals were purchased from commercial sources and used without further

purification. The ligands 4-amino-3,5-diisopropyl-1,2,4-triazole (4-NH_2-$\mathbf{L^{CH3}}$)[1] and *S*,*S* or *R*,*R*-4-amino-3,5-bis(1-hydroxyethyl)-1,2,4-triazole (*S*,*S* or *R*,*R*-4-NH_2-$\mathbf{L^{OH}}$)[2] were synthesized according to the literature procedures. Powder X-ray diffraction (PXRD) was carried out with an X-ray diffractometer of Rigaku, Rint 2000. The C, H, and N elemental analyses were conducted on a Perkin-Elmer 240C elemental analyzer. The FT-IR spectra were recorded from KBr pellets in the range 4000-400 cm^{-1} on a Mattson Alpha-Centauri spectrometer. Thermogravimetric analyses (TGA) were carried out on a Perkin-Elmer TG-7 analyzer heated from room temperature to 800 °C at a ramp rate of 5 °C/min under nitrogen. The solid-state circular dichroism (CD) spectra were recorded on a MOS-500 Spectrometer with KCl pellets.

S2. Synthesis

Synthesis of Conglomerate 1

A solid mixture of 4-NH_2-$\mathbf{L^{CH_3}}$ (100 mg, 0.59 mmol), $Cu(NO_3)_2 \cdot 3H_2O$ (150 mg, 0.62 mmol) was suspended in H_2O (8 ml) in a 15ml Teflon-lined stainless steel container. The mixture was heated in an isotherm oven at 160 °C for 72 h resulting in colorless crystals, which were isolated by washing with H_2O and ethanol. The sample was dried in air at room temperature overnight. Yield: 72% based on 1 mol of 4-NH_2-$\mathbf{L^{CH3}}$. Elemental analyses calcd (%) for $C_{24}H_{48}Cu_4N_{10}O_6$ (826.88): C, 34.86; H, 5.85; N, 16.94; Found C, 34.75; H, 5.93; N, 17.03. IR cm^{-1} (KBr): 3442 (w), 2962 (w), 2926 (m), 2864 (m), 1709 (s), 1639 (m) , 1512 (w), 1471 (w), 1440 (m), 1384 (w) , 1305 (m), 1276 (m), 1222 (s), 1169 (s), 1090 (m), 1048 (s), 925 (s), 833 (s), 772 (m), 539 (m).

Synthesis 2P (2M)

A solid mixture of *S*,*S*-4-NH_2-$\mathbf{L^{OH}}$ (100 mg, 0.58 mmol) (for **2M**, *R*,*R*-4-NH_2-$\mathbf{L^{OH}}$ was used), $Cu(NO_3)_2 \cdot 3H_2O$ (150 mg, 0.62 mmol) was suspended in H_2O (8 ml) in a 15ml Teflon-lined stainless steel container. The mixture was heated in an isotherm oven at 160 °C for 72 h resulting in colorless crystals, which were isolated by washing with H_2O and ethanol. The sample was dried in air at room temperature overnight. Yield: 68% based on 1 mol of *S*,*S*-4-NH_2-$\mathbf{L^{OH}}$. Elemental analyses calcd (%) for $C_{18}H_{36}Cu_4N_{10}O_{12}$ (838.73): C, 25.78; H, 4.33; N, 16.70; Found C, 25.67; H, 4.41; N, 16.53. IR cm^{-1} (KBr): 3385 (m), 2972 (m), 2921 (m), 1703 (s), 1629 (s), 1511 (m), 1473

(m), 1366 (m), 1313 (m), 1130 (m), 1074 (m), 1017 (m), 899 (s), 825 (s), 666 (s), 533 (s), 451 (s).

Synthesis of 1P(1M)

A solid mixture of 4-NH_2-$\mathbf{L^{CH_3}}$ (80 mg, 0.47 mmol), *S*,*S*-4-NH_2-$\mathbf{L^{OH}}$ (20 mg, 0.12 mmol) or L-alanine (45 mg, 0.5 mmol) or L-phenylglycine (75 mg, 0.5 mmol) (for **1M**, *R*,*R*-4-NH_2-$\mathbf{L^{OH}}$ or D-alanine or D-phenylglycine was used), $Cu(NO_3)_2 \cdot 3H_2O$ (120 mg, 0.50 mmol) was suspended in H_2O (8 ml) in a 15ml Teflon-lined stainless steel container. The mixture was heated in an isotherm oven at 160 °C for 72 h resulting in colorless crystals, which were isolated by washing with H_2O and ethanol. The sample was dried in air at room temperature overnight. Yield: 75% based on 1 mol of 4-NH_2-$\mathbf{L^{CH_3}}$. Elemental analyses calcd (%) for $C_{24}H_{48}Cu_4N_{10}O_6$ (826.88): C, 34.86; H, 5.85; N, 16.94; Found C, 34.91; H, 5.77; N, 16.85.

S3. Proton conductivity measurements

The powders were prepared by grinding the sample into a homogeneous powder with a mortar and pestle. With a press and a die measuring 10 mm in diameter and 0.95 mm (±0.05%) in thickness, samples of **1** and **2** were pressed into disk-shaped pellets. The impedances were measured with a frequency response analyzer/potentiostat (IviumStat) over a frequency range from 1 Hz to 1 MHz, with a two probe electrochemical cell and an applied ac voltage of 50 mV. Measurements were taken in the temperature range of 25–55 °C with 65% relative humidity and in the relative humidity range of 33%–97% at 25 °C (controlled by using an BPHS-060A incubator), respectively. The Nyquist plot obtained from impedance measurement comprises a depressed semicircular arc at high frequency and a spur at low frequency. The high frequency arc can be attributed to the bulk electrolyte resistance and the low frequency spur is possibly related to electrode-electrolyte interfacial impedance. The resistance values are estimated by extrapolation of the high frequency arc crossing to the real axis. Conductivity was calculated using the following equation:

$\sigma = L / RS$

where σ is the conductivity (S cm^{-1}), L is the measured sample thickness (cm), S is the

electrode area (cm^2) and R is the impedance (Ω).

S4. X-ray crystallography study

Single-crystal X-ray diffraction data were recorded on a Bruker Apex CCD diffractometer with graphite-monochromated Mo*Kα* radiation ($\lambda = 0.71069$ Å) at 293K. Absorption corrections were applied using multi-scan technique. All the structures were solved by Direct Method of SHELXS-97[3] and refined by full-matrix least-squares techniques using the SHELXL-2016[4] program within WinGX.[5] Non-hydrogen atoms were refined with anisotropic temperature parameters. During the refinement, the restraint commands "SIMU", "DELU" and "DFIX" were used to the isopropyl or 1-hydroxyethyl group on the 3 and 5-position of triazole ring to make the thermal parameters and geometry parameters of atoms crystallographically and chemically reasonable. For all the structures, some residual electron densities, which should be considered as peaks from disordered water molecules and counter anions, do not give a chemical meaningful result after a careful refinement. Therefore, the contributions of the disordered solvent molecules and anions were removed from the diffraction data using the SQUEEZE routine of the latest PLATON software[6] and the structures were then refined again using the data generated. The platon.sqf files were attached to the CIF files. These electron densities account to *ca.* twelve water molecules and four NO_3^- anions in the unit cell, which are directly added into the final formula, and these molecules are further estimated by TGA analysis combining with element analysis; The detailed crystallographic data and structure refinement parameters for **1P/1M** and **2P/2M** are summarized in Table S1, supporting information. Selected bond lengths and angles for these complexes are given in Tables S2. Crystallographic data for the structures reported in this paper have also been deposited with the CCDC as deposition no. CCDC 1423660 (**1P**), 1423661 (**1M**), 1423662 (**2M**), 1423663 (**2P**)(available free of charge, on application to the CCDC, 12 Union Rd., Cambridge CB2 1EZ, U.K.; e-mail deposit@ccdc.cam.ac.uk).

Table S1. Crystal data and refinement parameters for compounds **1P**, **1M**, **2P** and **2M**

Compound reference	**1P**	**1M**	**2P**	**2M**

Chemical formula	$C_{24}H_{48}Cu_4N_{10}O_6$	$C_{24}H_{48}Cu_4N_{10}O_6$	$C_{18}H_{36}Cu_4N_{10}O_{12}$	$C_{18}H_{36}Cu_4N_{10}O_{12}$
Formula Mass	826.88	826.88	838.73	838.73
Crystal system	Hexagonal	Hexagonal	Hexagonal	Hexagonal
a/(Å)	19.603(5)	19.593(4)	19.613(3)	19.6977(13)
b/(Å)	19.603(5)	19.593(4)	19.613(3)	19.6977(13)
c/(Å)	13.939(5)	13.927(3)	13.849(3)	13.8757(10)
α/°	90	90	90	90
β/°	90	90	90	90
γ/°	120	120	120	120
Unit cell volume/(Å)^3	4639(3)	4630(2)	4613.6(16)	4662.5(7)
Temperature/K	100(2)	100(2)	100(2)	293(2)
Space group	$P6_322$	$P6_322$	$P6_322$	$P6_322$
No. of formula units per unit cell, *Z*	4	4	4	4
Theta range for data collection (degree)	1.89 to 24.76	1.89 to 25.10	1.89 to 25.10	1.19 to 25.07
No. of reflections measured	26376	27090	26991	27099
No. of independent reflections	2670	2774	2759	2785
Completeness to theta	99.8%	99.8%	99.6%	99.7%
Data / restraints / parameters	2670 / 48 / 113	2774 / 48 / 113	2759 / 66/ 113	2785 /90 / 113
R_{int}	0.0701	0.0737	0.0909	0.0759
Final R_1 values ($I > 2\sigma(I)$)[a]	0.0475	0.0482	0.0583	0.0566
Final $wR(F^2)$ values ($I > 2\sigma(I)$)[b]	0.1204	0.1264	0.1581	0.1424
Final R_1 values (all data)	0.0709	0.0737	0.0932	0.0782
Final $wR(F^2)$ values (all data)	0.1332	0.1416	0.1785	0.1507
Flack parameter	0.034(17)	0.046(18)	0.04(2)	0.06(2)
Goodness of fit on F^2	1.028	1.006	1.058	1.006

[a] $R_1=\Sigma||F_o|-|F_c||/\Sigma|F_o|$. [b] $wR_2= |\Sigma w(|F_o|^2-|F_c|^2)|/\Sigma|w(F_o^2)^2|^{1/2}$

Table S2. Selected bond lengths (Å) and bond angles (°)

Bond lengths (Å)			
1P		**1M**	
Cu(1)-N(1)#1	1.940(6)	Cu(1)-N(1)	1.938(8)
Cu(1)-N(1)	1.940(6)	Cu(1)-N(1)#1	1.938(8)
Cu(1)-N(1)#2	1.940(6)	Cu(1)-N(1)#2	1.938(8)
Cu(2)-N(2)	1.850(5)	Cu(2)-N(2)	1.849(7)
Cu(2)-N(2)#3	1.850(5)	Cu(2)-N(2)#3	1.849(7)
Cu(3)-N(3)	1.863(6)	Cu(3)-N(3)#4	1.867(8)
Cu(3)-N(3)#4	1.863(6)	Cu(3)-N(3)	1.867(8)
Bond angles (°)			
1P		**1M**	
N(1)#1-Cu(1)-N(1)	119.977(10)	N(1)-Cu(1)-N(1)#1	119.979(12)
N(1)#1-Cu(1)-N(1)#2	119.975(10)	N(1)-Cu(1)-N(1)#2	119.979(12)
N(1)-Cu(1)-N(1)#2	119.976(12)	N(1)#1-Cu(1)-N(1)#2	119.978(15)
N(2)-Cu(2)-N(2)#3	177.8(4)	N(2)-Cu(2)-N(2)#3	177.9(5)
N(3)-Cu(3)-N(3)#4	179.9(4)	N(3)#4-Cu(3)-N(3)	179.6(6)
C(1)-N(1)-Cu(1)	134.7(5)	C(9)-N(2)-Cu(2)	135.4(7)
N(2)-N(1)-Cu(1)	117.8(4)	N(1)-N(2)-Cu(2)	117.8(6)
C(2)-N(2)-Cu(2)	135.3(5)	C(9)-N(3)-Cu(3)	126.9(8)
N(1)-N(2)-Cu(2)	118.4(4)	C(1)-N(3)-Cu(3)	127.5(7)
C(1)-N(3)-Cu(3)	127.1(6)	C(1)-N(1)-Cu(1)	134.8(4)
C(2)-N(3)-Cu(3)	127.3(5)	N(2)-N(1)-Cu(1)	117.8(6)
Symmetry transformations used to generate equivalent atoms:		Symmetry transformations used to generate equivalent atoms:	
#1 -x+y,-x+1,z #2-y+1,x-y+1,z #3 -x+y,y,-z+1/2 #4-x,-x+y,-z+1		#1 -y+1,x-y+1,z #2 -x+y,-x+1,z #3 -y+1,-x+1,-z+3/2 #4 x-y+1,-y+2,-z+1	

Table S3-1. A summary of structure determinations of ten randomly selected crystals for **2P** synthesized from *S*,*S*-$\mathbf{L^{OH}}$: Cell parameters, R factors, Flack absolute structure parameters for each refinement in $P6_322$ space group and observed helicity are given.

SN	*a*	*c*	R_1	wR_2	Flack parameter	Helicity
1	19.6758(8)	13.7959(8)	0.0518	0.1492	0.02(5)	P
2	19.6895(3)	13.8220(2)	0.0610	0.1245	0.05(3)	P
3	19.6952(5)	13.8303(4)	0.0553	0.1376	0.00(2)	P
4	19.6865(11)	13.7989(13)	0.0578	0.1236	0.06(5)	P
5	19.6654(6)	13.8648(6)	0.0486	0.1308	-0.02(9)	P
6	19.6797(14)	13.8287(9)	0.0565	0.1148	0.04(2)	P
7	19.6969(8)	13.8115(5)	0.0478	0.1405	0.01(6)	P
8	19.6855(10)	13.7607(11)	0.0490	0.1237	0.06(4)	P
9	19.6903(4)	13.7738(4)	0.0603	0.1522	0.05(2)	P
10	19.6916(7)	13.8290(7)	0.0499	0.1246	0.08(3)	P

Table S3-2. A summary of structure determinations of ten randomly selected crystals for **2M** synthesized from *R*,*R*-$\mathbf{L^{OH}}$: Cell parameters, R factors, Flack absolute structure parameters for each refinement in $P6_322$ space group and observed helicity are given.

SN	*a*	*c*	R_1	wR_2	Flack parameter	Helicity
1	19.6952(8)	13.8808(8)	0.0501	0.1447	0.04(2)	M
2	19.6891(6)	13.8596(6)	0.0565	0.1606	0.00(3)	M
3	19.6754(9)	13.8138(12)	0.0480	0.1504	0.05(2)	M
4	19.6902(5)	13.8752(5)	0.0574	0.1562	0.08(4)	M
5	19.6848(4)	13.8404(4)	0.0438	0.1402	-0.01(7)	M
6	19.6738(7)	13.8344(7)	0.0610	0.1373	0.02(4)	M
7	19.6693(13)	13.7816(12)	0.0603	0.1569	0.03(6)	M
8	19.6722(3)	13.7696(6)	0.0555	0.1324	0.00(5)	M
9	19.6915(5)	13.8308(4)	0.0539	0.1271	0.03(2)	M
10	19.6879(8)	13.8097(6)	0.0473	0.1593	0.07(5)	M

Table S4. A summary of structure determinations of ten randomly selected crystals for **1** grown in the absence of any enantiopure sources: Cell parameters, R factors, Flack absolute structure parameters for each refinement in $P6_322$ space group and observed helicity are given.

SN	*a*	*c*	R_1	wR_2	Flack parameter	Helicity
1	19.5846(7)	13.9061(7)	0.0538	0.1282	-0.02(10)	M
2	19.5986(10)	13.8723(12)	0.0446	0.1238	0.01(3)	M
3	19.6132(5)	13.8768(5)	0.0488	0.1543	0.07(5)	M
4	19.586(8)	13.961(5)	0.0546	0.1164	0.02(3)	M
5	19.6158(3)	13.9171(6)	0.0609	0.1413	0.03(2)	M
6	19.5988(2)	13.9534(3)	0.0555	0.1333	-0.01(5)	P
7	19.5762(11)	13.9043(2)	0.0587	0.1369	0.04(8)	P
8	19.6077(8)	13.9691(8)	0.0465	0.1257	0.06(7)	P
9	19.5988(6)	13.8834(6)	0.0583	0.1488	0.05(4)	P
10	19.6034(2)	13.9402(8)	0.0562	0.1507	0.04(3)	P

Table S5. A summary of structure determinations of ten randomly selected crystals for **1P** grown in the presence of *S*,*S*-$\mathbf{L^{OH}}$: Cell parameters, R factors, Flack absolute structure parameters for each refinement in $P6_322$ space group and observed helicity are given.

SN	*a*	*c*	R_1	wR_2	Flack parameter	Helicity
1	19.5835(10)	13.8968(10)	0.0500	0.1630	0.06(2)	p
2	19.6133(3)	13.8906(3)	0.0605	0.1319	-0.03(7)	p
3	19.5954(7)	13.9549(7)	0.0532	0.1415	0.05(4)	p
4	19.5919(5)	13.9388(8)	0.0484	0.1548	0.08(3)	p
5	19.6025(3)	13.9292(4)	0.0476	0.1497	0.04(3)	p
6	19.5850(12)	13.8836(4)	0.0557	0.1617	0.03(5)	P
7	19.589(8)	13.866(8)	0.0503	0.1379	-0.02(10)	P
8	19.6098(5)	13.8950(5)	0.0612	0.1312	0.05(2)	P
9	19.6184(6)	13.8949(7)	0.0593	0.1479	0.07(3)	P
10	19.5862(2)	13.9100(2)	0.0602	0.1383	0.05(8)	P

Table S6. A summary of structure determinations of ten randomly selected crystals for **1M** grown in the presence of *R*,*R*-$\mathbf{L^{OH}}$: Cell parameters, R factors, Flack absolute structure parameters for each refinement in $P6_322$ space group and observed helicity are given.

SN	*a*	*c*	R_1	wR_2	Flack parameter	Helicity
1	19.6015(3)	13.8680(9)	0.0521	0.1486	0.06(9)	M
2	19.5941(12)	13.9360(5)	0.0709	0.1451	0.04(3)	M
3	19.5753(5)	13.8752(5)	0.0495	0.1237	-0.07(11)	M
4	19.6046(3)	13.8958(3)	0.0467	0.1250	0.05(3)	M
5	19.5851(8)	13.9012(8)	0.0604	0.1414	0.00(5)	M
6	19.6125(2)	13.9226(9)	0.0471	0.1247	0.01(6)	M
7	19.6123(10)	13.8858(10)	0.0527	0.1470	0.04(2)	M
8	19.591(4)	13.905(5)	0.0564	0.1480	0.05(4)	M
9	19.6031(2)	13.9173(2)	0.0469	0.1636	0.03(2)	M
10	19.5873(14)	13.8931(12)	0.0515	0.1171	0.06(7)	M

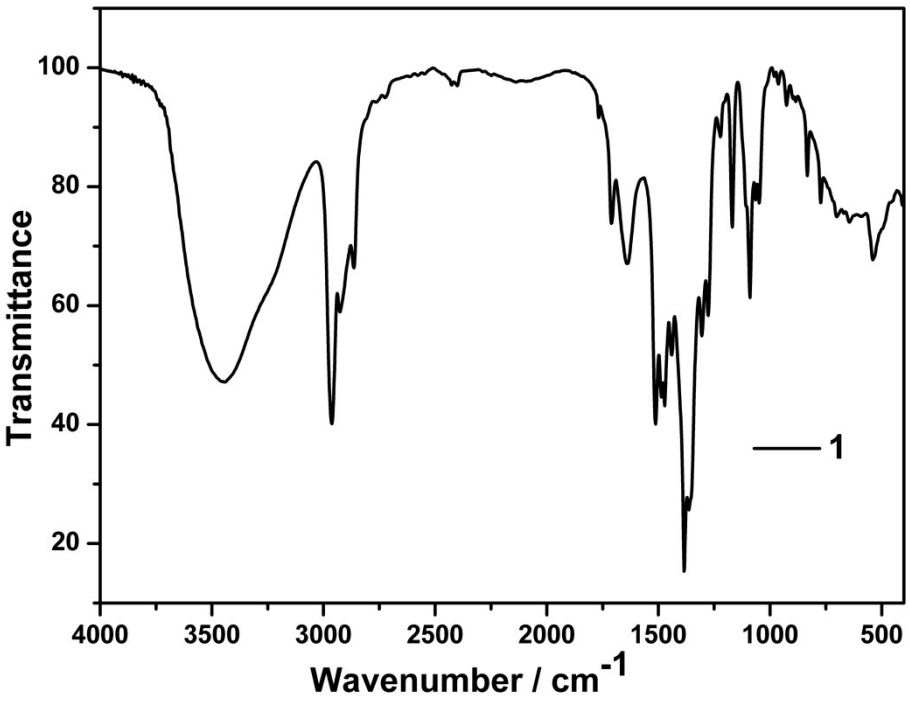

Figure S1-1. Infrared spectrum of fresh **1**

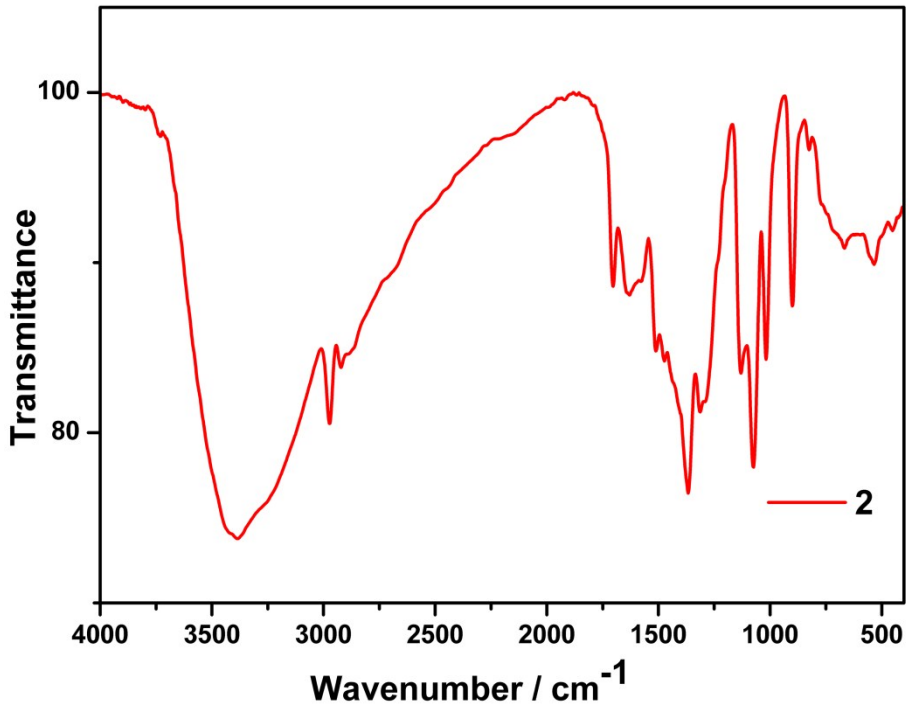

Figure S1-2. Infrared spectrum of fresh **2**

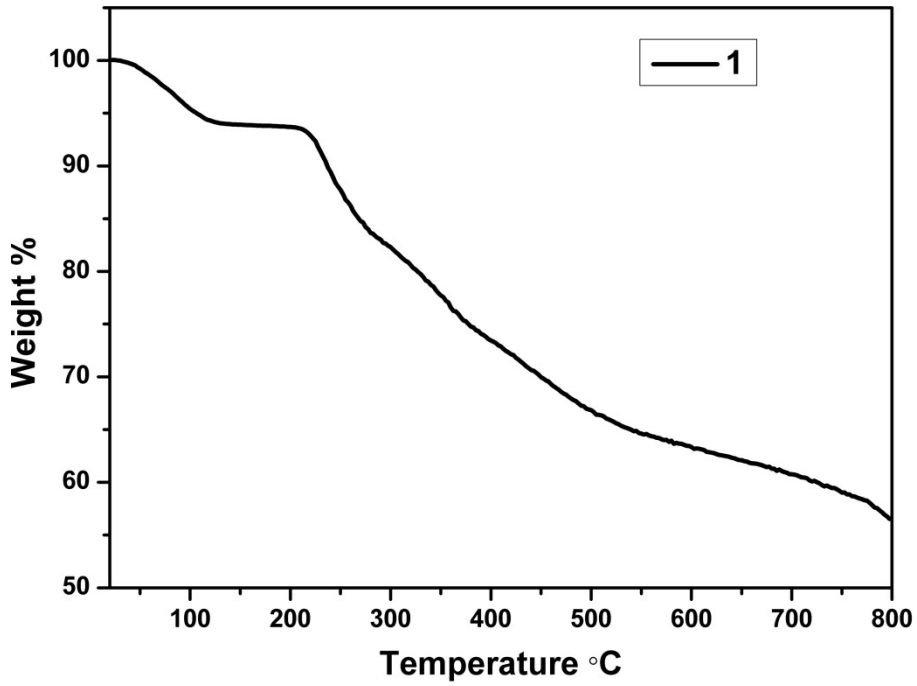

Figure S2-1. TGA curve of compound **1**

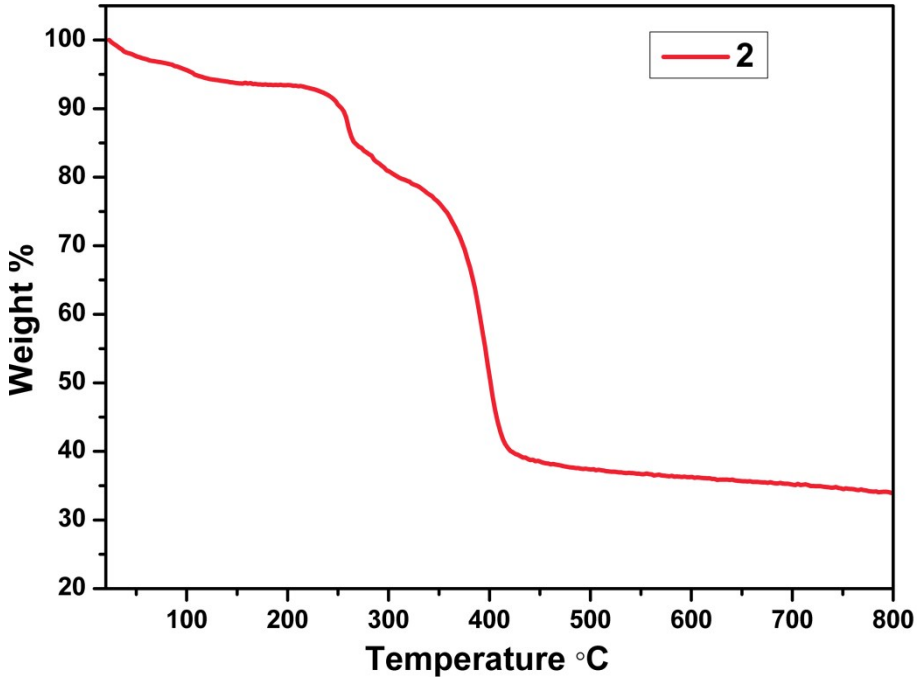

Figure S2-2. TGA curve of compound **2**

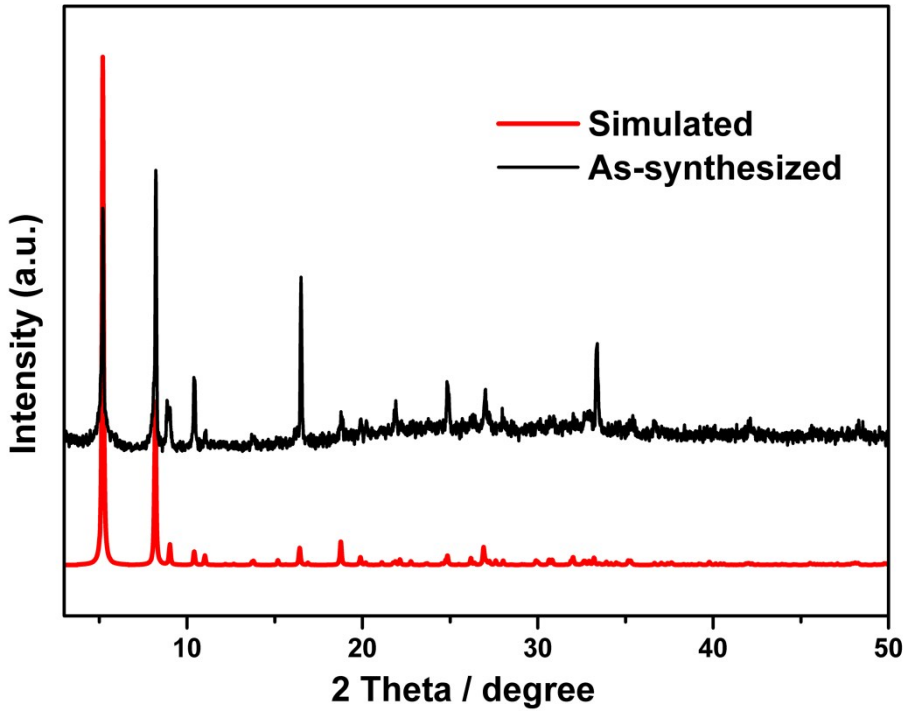

Figure S3-1. PXRD profiles of as-synthesized **1** and the simulated one

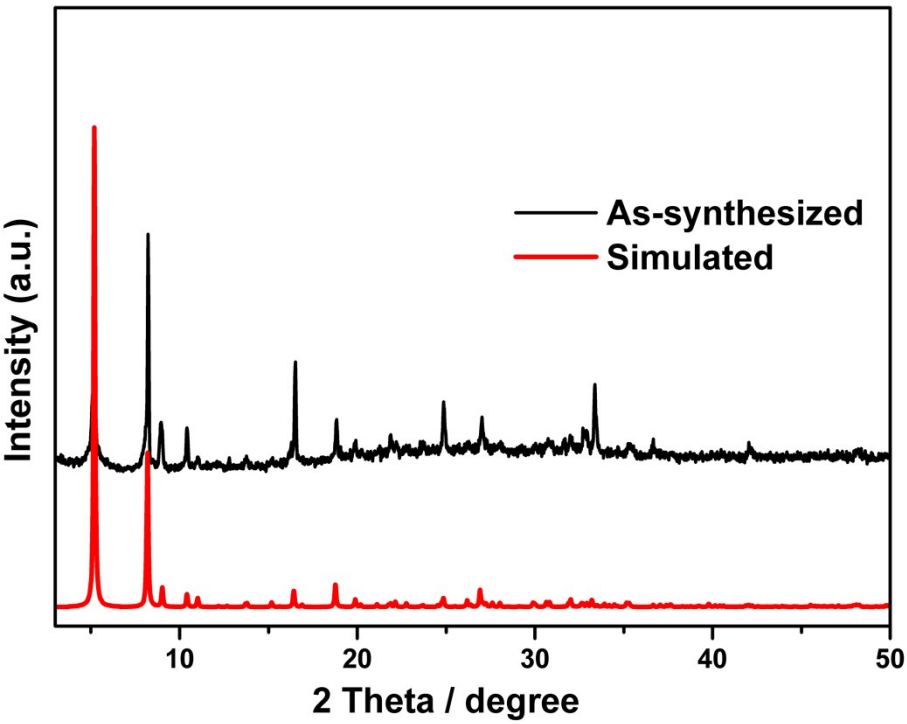

Figure S3-2. PXRD profiles of as-synthesized **2** and the simulated one.

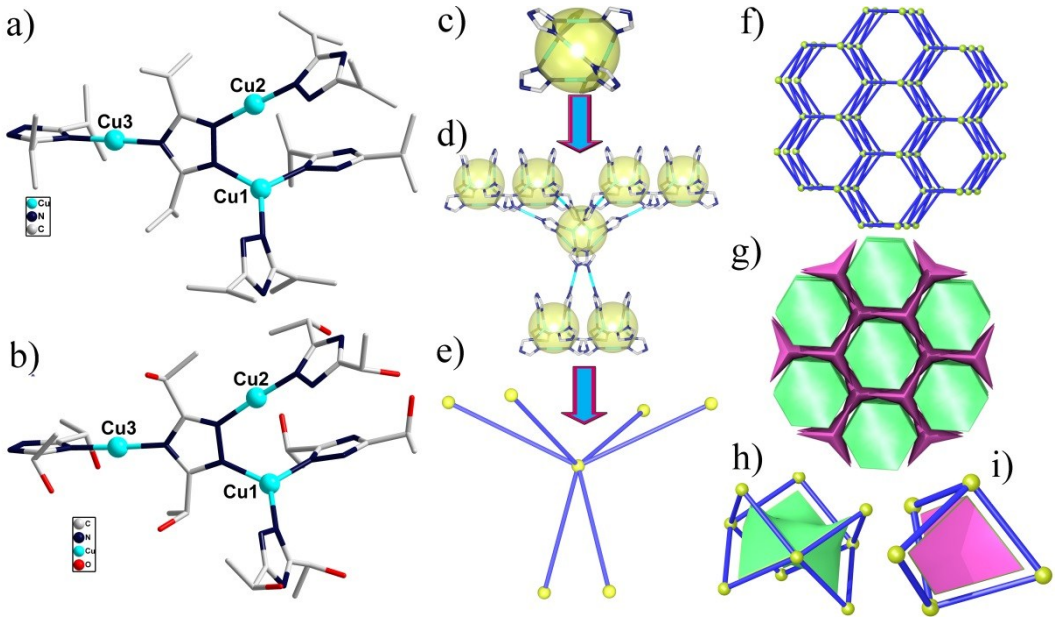

Figure S4. a) and b) The coordination environment for different Cu^{I} ions in **1P** and **2P**. c), d) and e) The propeller-like chiral $[Cu_5(L^{CH_3})_6]$ clusters are regarded as 6-connected nodes. f) The underlying intrinsically chiral acs topology. g) Tiling figure of **1** and **2**. The tiling shows one kind of vertices, one kinds of edge, two kinds of faces, and two kinds of tiles. h) and i) The two kinds of tiles in the tiling figure. All the hydrogen atoms have been omitted for clarity.

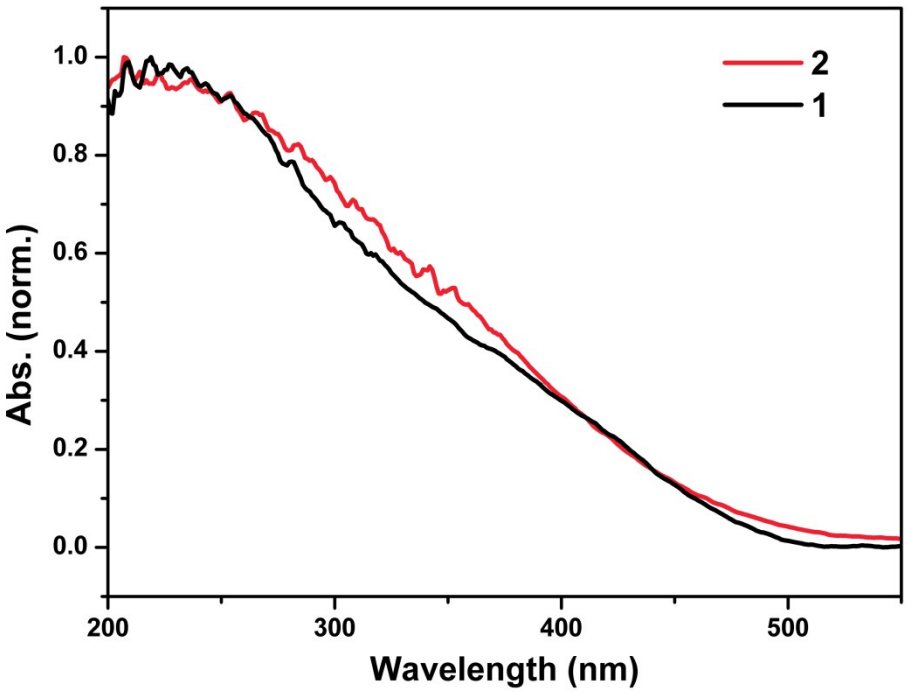

Figure S5. The UV-vis spectra of the crystal of **1** and **2**

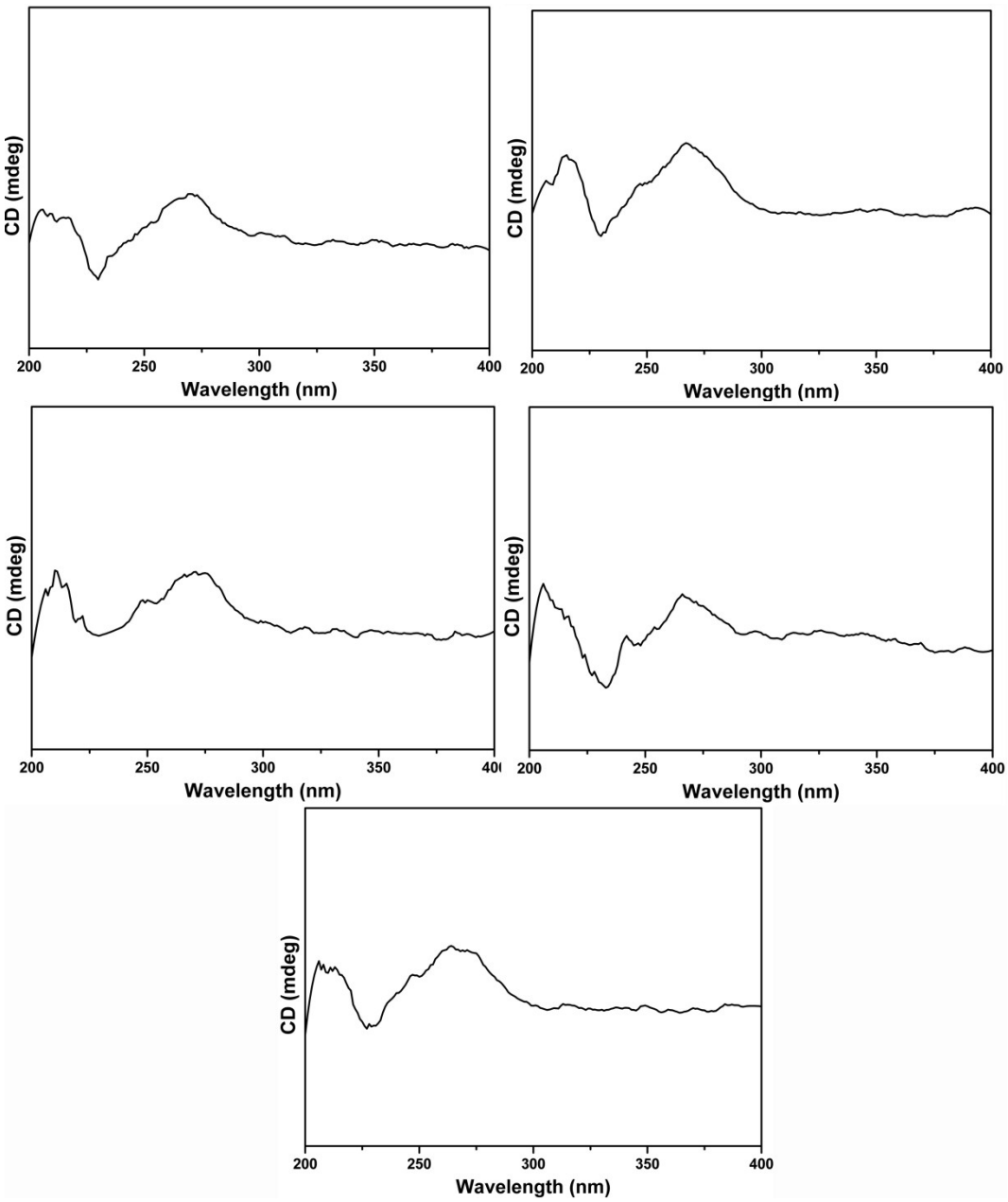

Figure S6-1. Solid state CD spectra recorded for five crystals of **2P** synthesized from *S*,*S*-$\mathbf{L}^{\mathbf{OH}}$. Positive dichroic signals approximately at 218 and 270 nm for all samples indicate the absolute formation of enantiomorph **2P**.

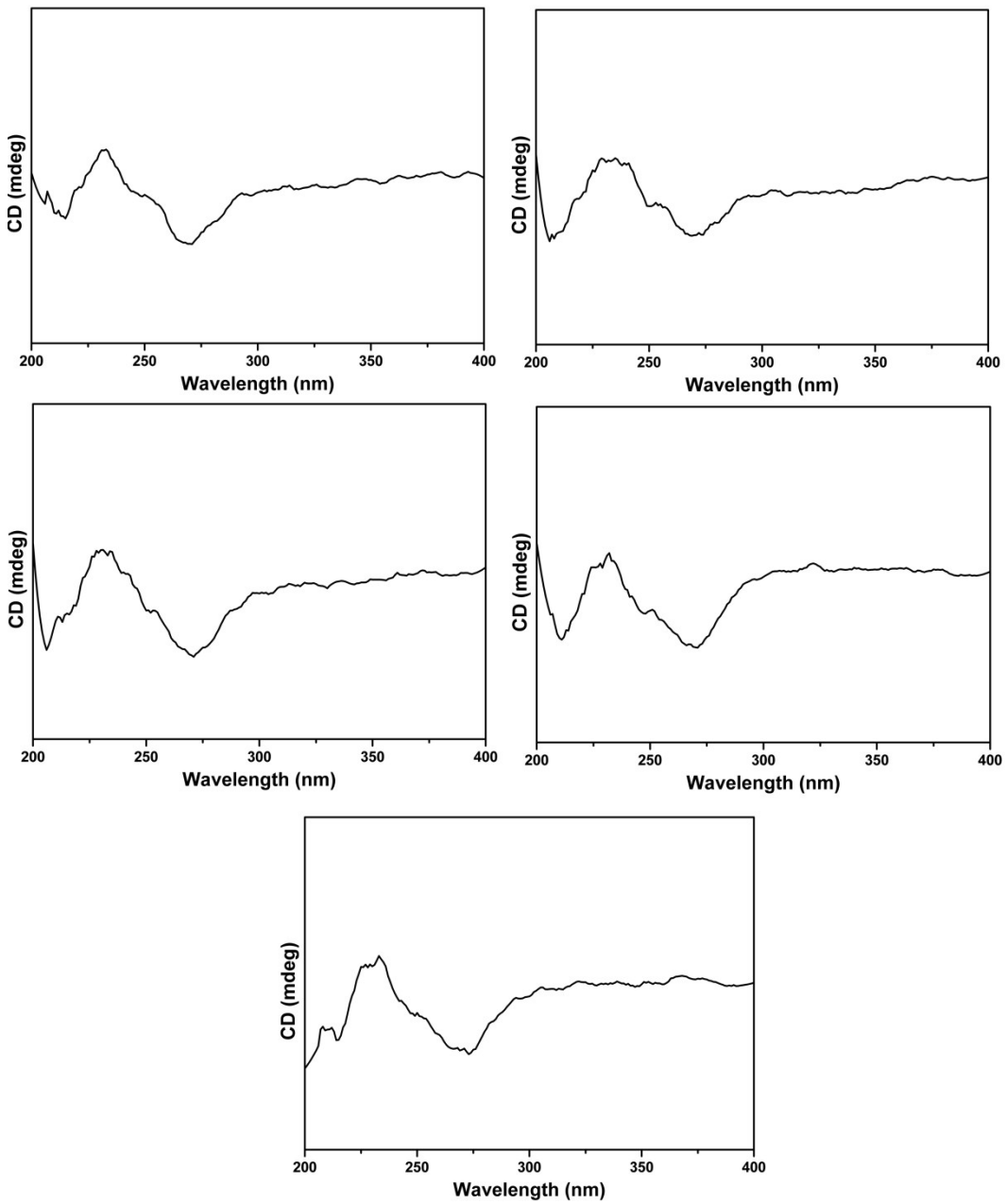

Figure S6-2. Solid state CD spectra recorded for five crystals of **2M** synthesized from *R*,*R*-$\mathbf{L}^{\mathbf{OH}}$. Negative dichroic signals approximately at 218 and 270 nm for all samples indicate the absolute formation of enantiomorph **2M**.

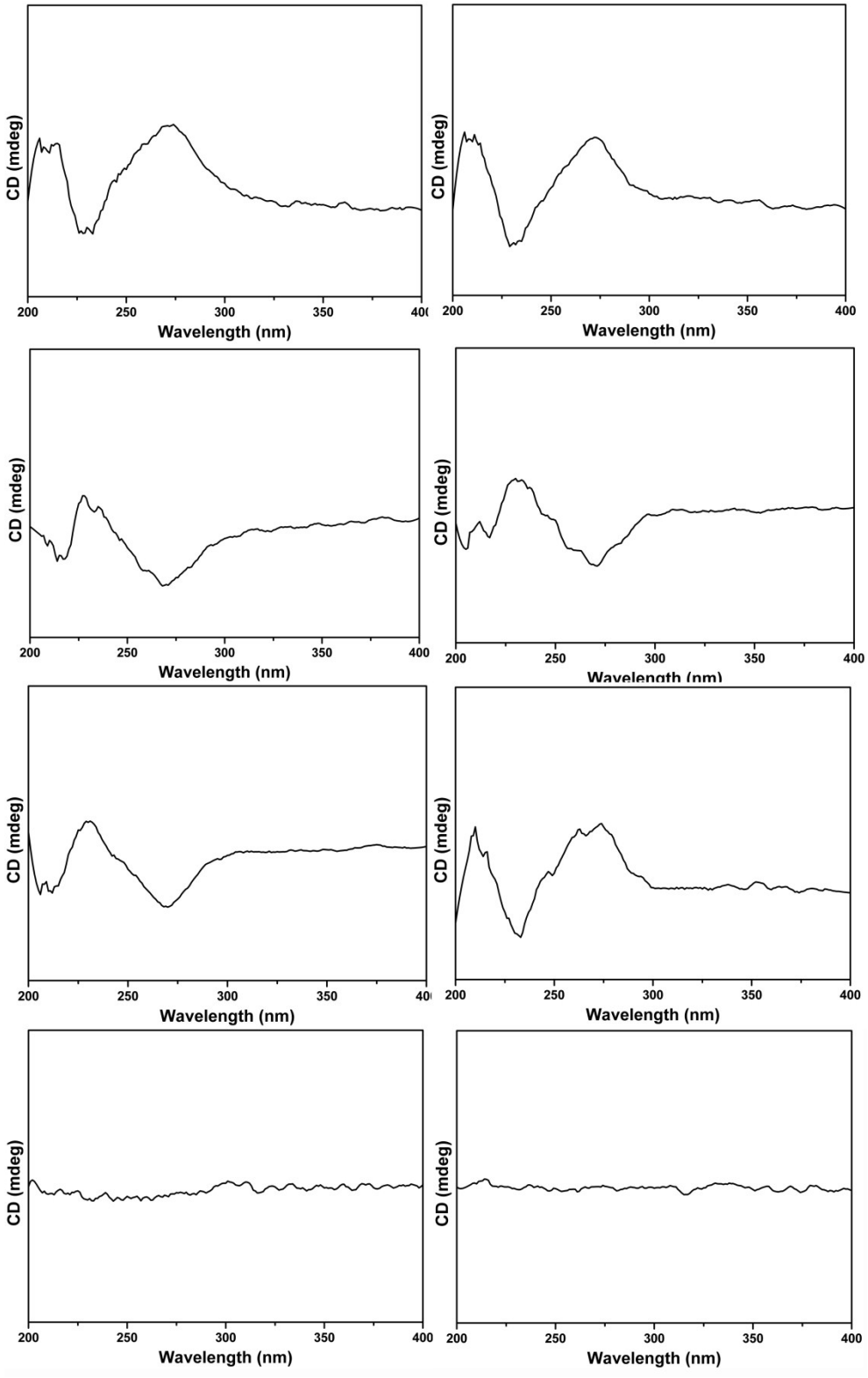

Figure S7. Solid state CD spectra recorded for single crystals and bulk samples of **1** grown in the absence of any enantiopure sources. The first six figures based on individual crystals show positive/negative dichroic signals varying from crystal to crystal, indicating the formation of a conglomerate. The last two figures based on bulk samples do not show any dichroic signals further reveal the formation of a conglomerate.

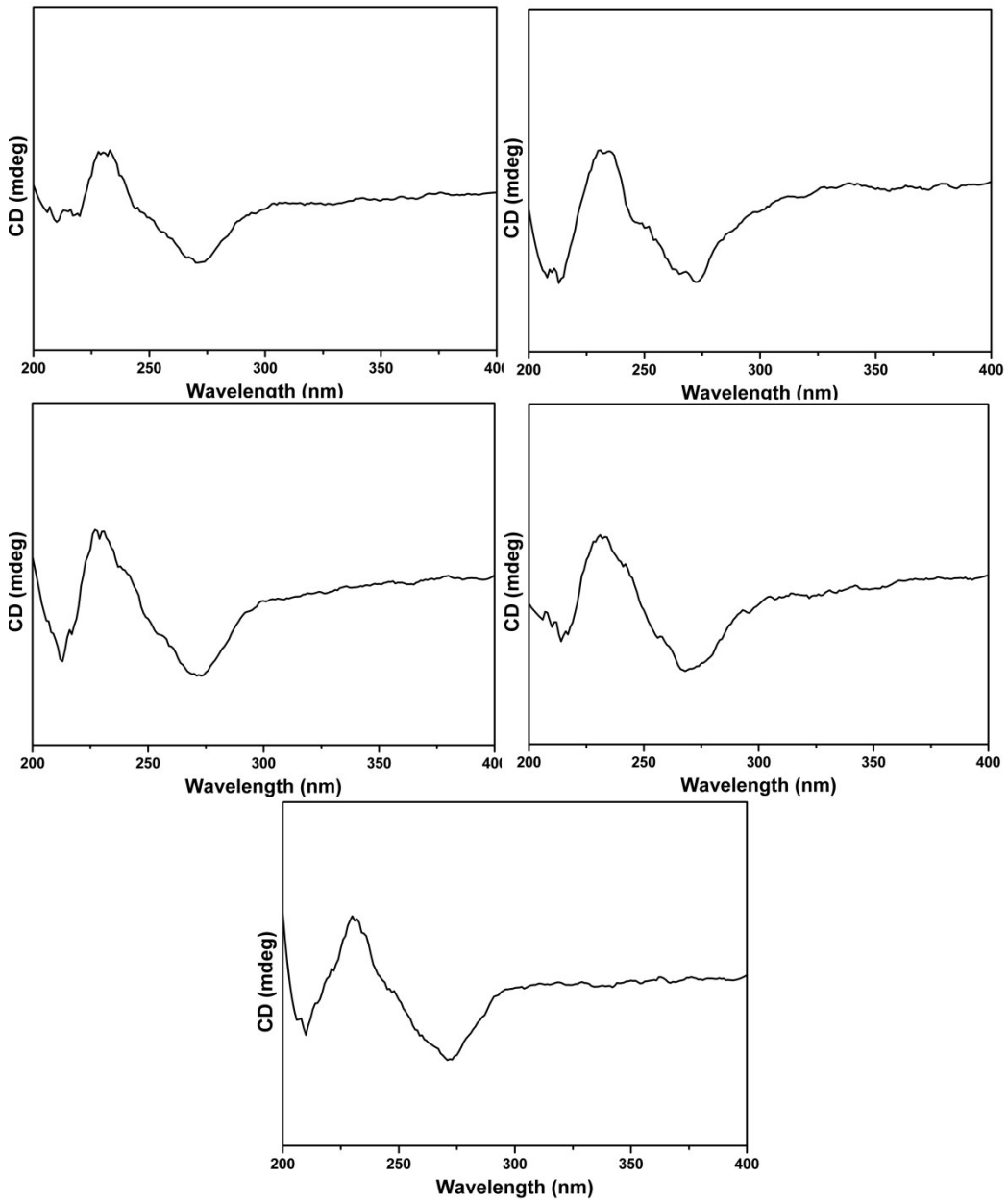

Figure S8. Solid state CD spectra recorded for bulk samples of **1** grown in the presence of *S*,*S*-$\mathbf{L^{OH}}$. Positive dichroic signals approximately at 218 and 270 nm for all samples indicate the exclusive formation of enantiomorph **1P**.

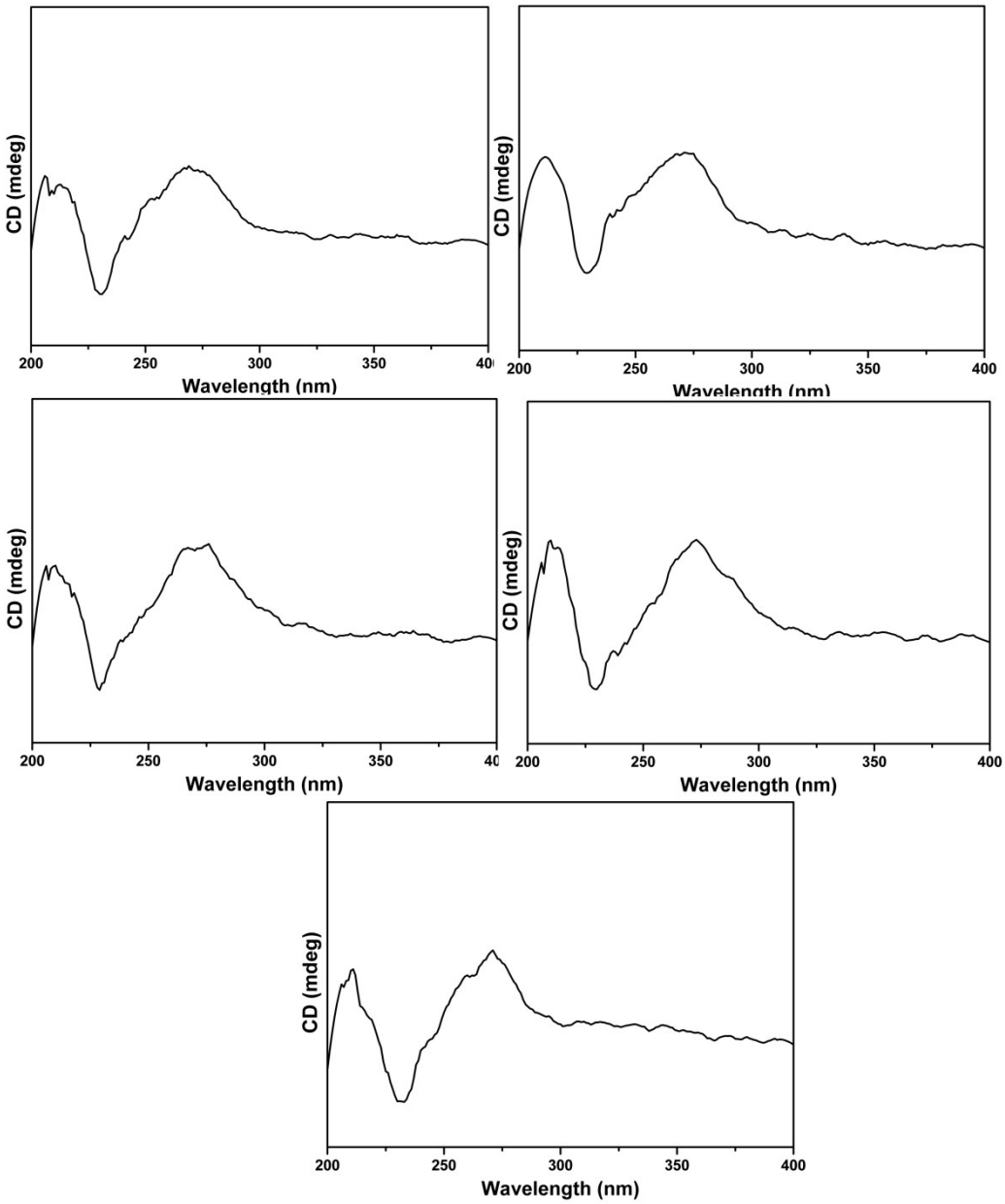

Figure S9. Solid state CD spectra recorded for bulk samples of **1** grown in the presence of *R*,*R*-$\mathbf{L^{OH}}$. Positive dichroic signals approximately at 218 and 270 nm for all samples indicate the exclusive formation of enantiomorph **1M**.

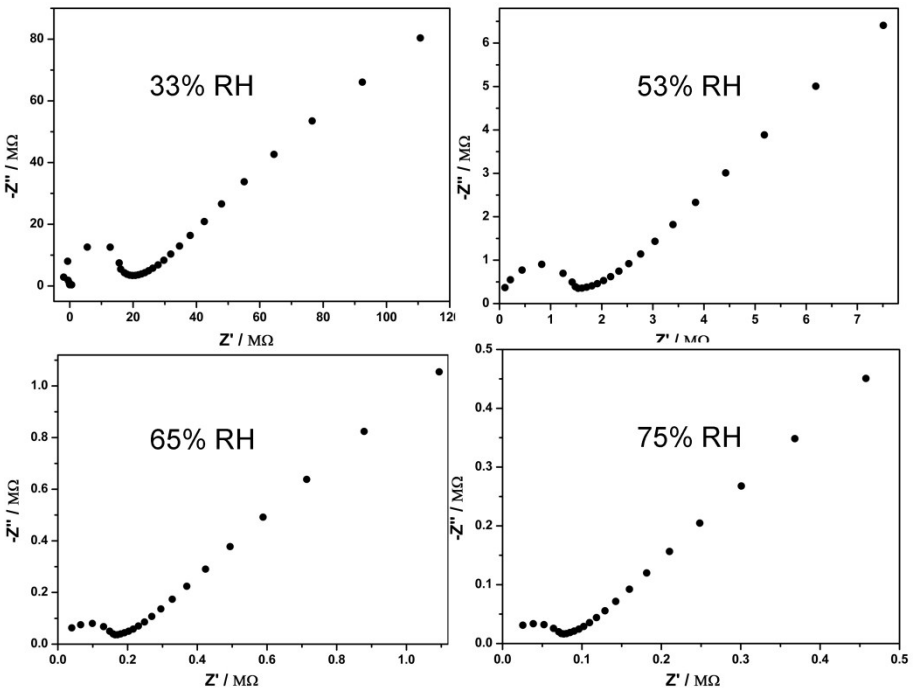

Figure S10-1. Impedance plots of **2** at 25 °C and different humidity conditions.

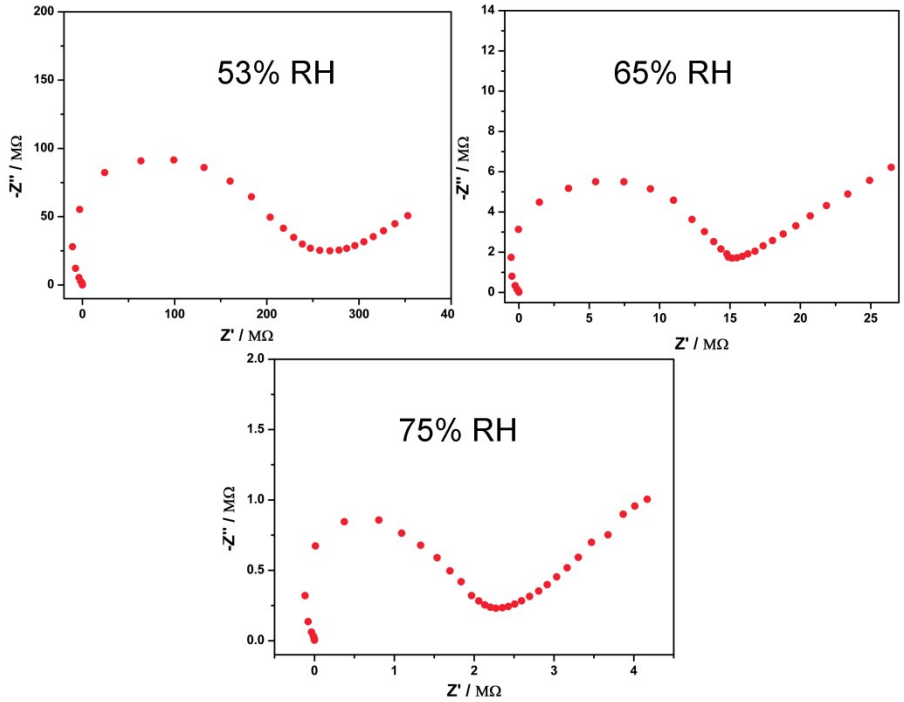

Figure S10-2. Impedance plots of **1** at 25 °C and different relative humidity conditions.

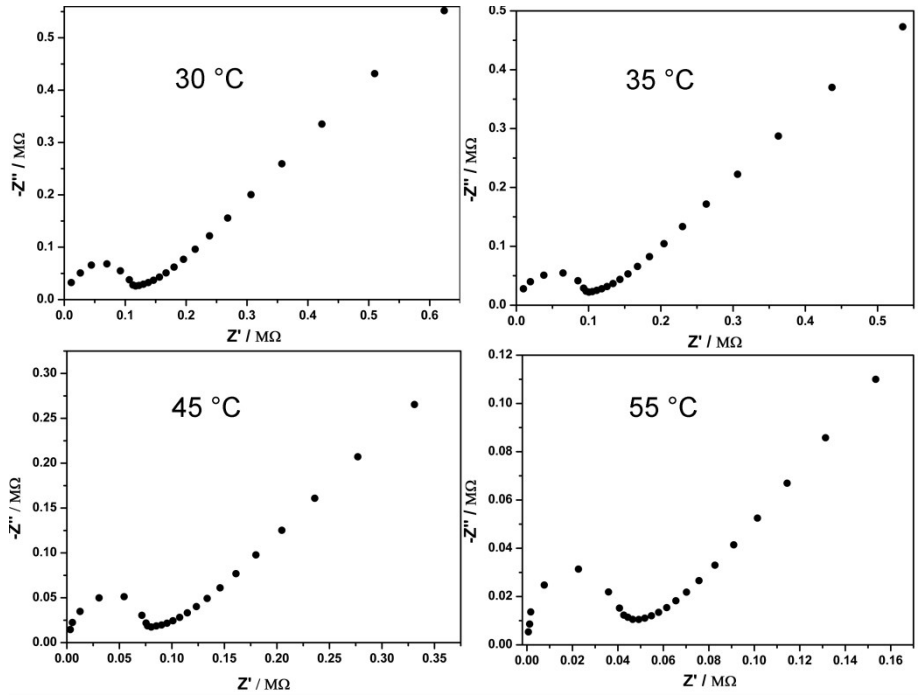

Figure S11-1. Impedance plots of **2** at 65% RH and different temperature.

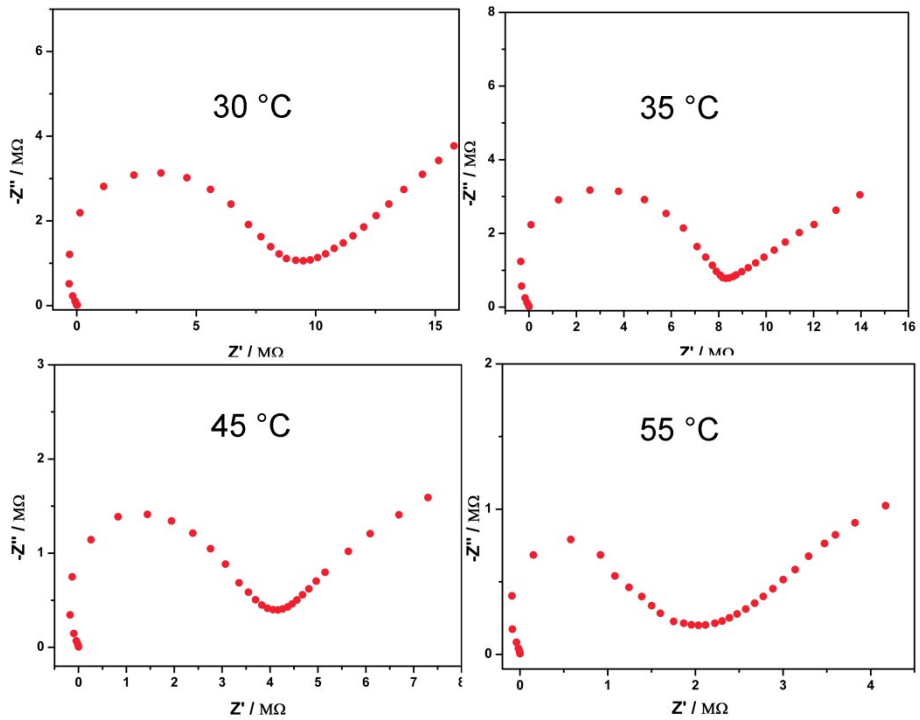

Figure S11-2. Impedance plots of **1** at 65% RH and different temperatures.

References:

1 G. Yang, P.-C. Duan, K.-G. Shi and R. G. Raptis, *Cryst. Growth Des.*, 2012, **12**, 1882.

2 (a) S. S. Iremonger, P. D. Southon and C. J. Kepert, *Dalton Trans.*, 2008, 6103; (b) J. Alonso, M. Martin, J. De Mendoza, T. Torres and J. Elguero, *Heterocycles*, 1987, **26**, 989.

3 G. M. Sheldrick, *SHELXS-97: Program for X-ray crystal structure solution;*, University of Göttingen:Göttingen, Germany, 1997.

4 G. M. Sheldrick, *Acta Crystallographica Section C*, 2015, **71**, 3.

5 L. J. Farrugia, *J. Appl. Crystallogr.*, 2012, **45**, 849.

6 A. L. Spek, *Acta Crystallographica Section C*, 2015, **71**, 9.